# Combined Unsupervised and Supervised Learning for Improving Chest X-Ray Classification

Anca Ignat and Robert-Adrian Găină
*Faculty of Computer Science, University "Alexandru Ioan Cuza" of Iaşi, Romania*

Keywords: Chest X-Ray, Pneumonia, Deep Learning Networks, Support Vector Machines (SVM), Random Forest (RF), Clustering Methods.

Abstract: This paper studies the problem of pneumonia classification of chest X-ray images. We first apply clustering algorithms to eliminate contradictory images from each of the two classes (normal and pneumonia) of the dataset. We then train different classifiers on the reduced dataset and test for improvement in performance evaluators. For feature extraction and also for classification we use ten well-known Convolutional Neural Networks (Resnet18, Resnet50, VGG16, VGG19, Densenet, Mobilenet, Inception, Xception, InceptionResnet and Shufflenet). For clustering, we employed 2-means, agglomerative clustering and spectral clustering. Besides the above-mentioned CNN, linear SVMs (Support Vector Machines) and Random Forest (RF) were employed for classification. The tests were performed on Kermany dataset. Our experiments show that this approach leads to improvement in classification results.

## 1 INTRODUCTION

Image processing methods allow us to perform some operations over an image in order to extract relevant information. One domain that highly benefits from this type of techniques is Medical Imaging. Medical images make up most of the data available in healthcare. CT, MRI and X-Ray are only some examples of files that are used for in-depth non-invasive exploration of internal anatomy. This way of transmitting data about a patient is available for medical staff to improve treatment.

The chest X-ray (CXR) is one of the most commonly accessible radiological examinations used in diagnosis lung diseases or respiratory symptoms. The benefits of this type of examinations that made it one of the most popular methods used even today are: cost-effectiveness, low radiation dose and ease of pathology detection from the results obtained.

Pneumonia is one of the most common lung diseases caused by viruses, bacteria or fungi. Pneumonia causes the inflammation of either one or both of the lungs with fluids that can cause cough and difficulty in breathing. When suffering from pneumonia, the exchange rate between carbon dioxide (CO2) and oxygen (O2) at the alveolar membrane level decreases. Pneumonia is treated based on the pathogen that caused the infection. Thus, for bacterial pneumonia antibiotics are used whilst for viral pneumonia antiviral drugs are administrated and antifungal drugs for the fungal pneumonia. Anyone can be affected by this disease though children and people over 65 are more susceptible of contacting it while lowering the chances of survival. A common approach used by radiologists in order to recognize a patient suffering from pneumonia is the analysis of a CXR. The main difference is based on the presence of white hazy regions that are not present in lungs of a healthy person.

The presence of pneumonia in the human body is a classification problem that radiologists face daily. However, due to a high demand in examinations and low number of experts able to give a diagnostic, there is a direct relation between the infection rate caused by pneumonia and the medical infrastructure available over a certain region[1]. Because of this, recent studies focused on developing classification models able to recognize pneumonia based on CXRs. The decisions usually made by medical staff can be helped by computer-aided diagnosis (CAD) tools that

[1] https://www.news-medical.net/health/Pneumonia-Epidemiology.aspx



Ignat, A. and Găină, R.
Combined Unsupervised and Supervised Learning for Improving Chest X-Ray Classification.
DOI: 10.5220/0011793000003417
In *Proceedings of the 18th International Joint Conference on Computer Vision, Imaging and Computer Graphics Theory and Applications (VISIGRAPP 2023) - Volume 4: VISAPP*, pages 475-482
ISBN: 978-989-758-634-7; ISSN: 2184-4321

can output a verdict based on the data given. A flow that a CAD system usually performs has three steps. In the first step, the CXR is pre-processed in order to prepare it for the next operations (Caseneuve et al., 2021). This implies resizing, reorienting or colour correcting operations in order to standardize images from multiple sources.

In the second step, features are extracted from the pre-processed image. The last step consists of analysing the features extracted in order to output a final result. Some relevant surveys that summarize recent progress in CXR image analysis are in (Khan, Zaki, Ali, 2021), (Çallı et al., 2021), (Li et al. 2020). In these papers one finds lists of datasets with CXR images, methods used for solving different types of problems that are CXR related and results obtained with several performance evaluators.

(Ayan and Ünver, 2019) use transfer learning and fine-tuning on Xception and VGG16 for detecting pneumonia. The tests are computed on Kermany (Kermany, Zhang, Goldbaum, 2018) dataset. In (Sharma, Jain, Bansal, 2020) different variations of a CNN architecture are presented with the use of neurons dropout. All the models with dropout outperform the normal model but the quality of the results depends on the probability of dropout. The experiments are performed on Kermany dataset with training and test sets different from those used in this article. (Hammoudi et al., 2021) compares VGG, Densenet and Inception Resnet tailored for the Kermany database in order to improve the results. After training, the model is also tested with a dataset containing CXR for adults, this dataset contains also the medical history of each person. It is shown that transfer learning can be efficient even if the data sources are differently collected. In (Mabrouk et al., 2022) the authors combine the results computed with three neural networks to improve the pneumonia classification results. They use Kermany dataset for their computations. In (Kundu et al., 2021) the authors also use ensemble methods with three neural networks and test their method on Kermany and RSNA datasets. The experiments are performed with a 5-fold cross-validation procedure. (Couhan et al., 2020) propose five models in order to classify the same dataset that is discussed in this paper and after analysing the results another meta-model that combines the previous ones achieves state-of-the art performance for the problem proposed, on Kermany dataset. (Zhang et al., 2021) present an analysis of the performance for different CNN architectures. They pre-process the dataset and develop a smaller VGG-like architecture for solving the pneumonia detection problem. They use Kermany dataset with a random split 70% for training, 10% for validation and 20% for testing.

The main novelty of our work is the use of clustering methods for the training set improvement, and thus, obtaining better classification results.

The article has five sections. The first presents the problem and the related work. The second section presents the Kermany dataset employed in the experiments. The clustering methods, the feature extraction process, the classification procedure and the methodology of combining them are described in Section 3. Section 4 is dedicated to the results of our tests. The final section presents conclusions and future directions of research.

## 2 DATASET

We used in our tests the Kermany dataset (Kermany, Zhang, Goldbaum, 2018). This dataset was downloaded from Kaggle[2]. This is a data collection of grayscale chest X-ray images. The images are in JPEG format, the sizes of these images are variable. The dataset is divided in three folders: test, val and train. In each of these folders there are two directories, labelled “normal” and “pneumonia”. We merged the train and val folders thus obtaining a training set with 1349 chest X-ray images of normal lungs and 3883 images for lungs affected by pneumonia. In the test set there are 234 images labelled “normal” and 390 with “pneumonia”. We did not apply any pre-processing enhancement method.

In Fig. 1 are two samples of images from this dataset, the first is a chest X-ray for normal lungs and the second is for lungs with pneumonia.

## 3 METHODS

The idea behind our computations is based on the observation that on the same medical image different physicians can establish different diagnostics. When working with medical image datasets, the images have one label, not always knowing how this label was settled.

[2] https://www.kaggle.com/datasets/paultimothymooney/chest-xray-pneumonia

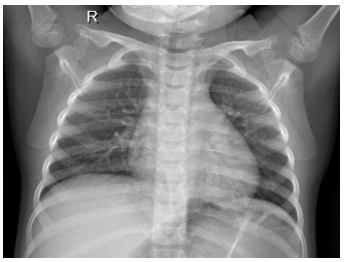


Normal lung chest X-ray image

Pneumonia affected lung chest X-ray image

Figure 1: Samples of images from the Kermany dataset.

In order to increase the coherence of the dataset, we intend to apply clustering methods on the training set of images, without taking into account the original labels of these images. We hope that the clustering algorithms will grasp hidden patterns in the CXR images, patterns that better define the differences between the healthy lungs and the pneumonia affected lungs.

The clustering methods are applied for dividing the training set in two clusters. Then, we retain in a given class, only the images that were also selected by the clustering algorithm. Thus, one obtains a reduced training set, assumingly more consistent than the original one. We consider that the new content of the two classes is formed by images which are better representatives of the modelled reality.

In this work we tested three clustering techniques. The first is k-means (in our case, 2-means) with two distances, Euclidean and Manhattan (Tan, Steinbach, and Kumar, 2019). The second algorithm is agglomerative clustering, with four types of cluster distances (Landau et al., 2011). The third technique is spectral clustering (Wierzchoń and Kłopotek, 2018).

The k-means algorithm is an iterative method that starts with k initial points and then it aggregates the data around these points. One computes the centroids of these clusters and computes a new cluster distribution. The process iterates until a certain cohesion criteria is fulfilled or a maximal number of iteration is achieved.

The agglomerative clustering starts with a number of clusters equal with the number of points in data. Then it aggregates two of these clusters that are at a minimum distance. At each step one has at least one cluster less than at the previous step. The process stops when the required number of clusters is achieved. The resulting clusters content depends on the chosen distance between clusters. We used four distances. For the first, the distance between clusters is given by the closest points of the two clusters. This method is called single linkage. The second distance is defined by the furthest points (complete linkage), the third computes the distance by averaging all the distances of points from different clusters (average linkage). The forth method of computing a distance measure between clusters is called Ward distance and depends on the centroids of the two clusters and the number of elements in each cluster.

The spectral clustering algorithm is a technique borrowed from graph theory, where the nodes are grouped in separate sets by computing eigenvalues and eigenvectors of the Laplacian matrix associated to the graph and keeping a reduced number of the eigenvalues, eigenvectors. In our particular situation, the nodes of the graph are the CXR images, the edges are defined by the similarity matrix (or distance matrix) between the images in the training set, this matrix is considered a generalized adjacency matrix for the graph.

We tested all these clustering algorithms on our dataset, and in all computations the single linkage algorithm performed poorly, one of the clusters having very few or no elements. Thus, we do not provide in this paper results for this clustering technique.

For applying clustering methods one needs features for image characterization. For this purpose, we first trained several well-known neural networks on the given dataset. We used two methods from the Resnet family, Resnet18 and Resnet50 (He, Zhang, Ren, Sun, 2016), two VGG networks, VGG16 and VGG19 (Simonyan, Zisserman, 2014), three Inception type methods, Inception v3, Xception, and InceptionResnet v2 (Szegedy et al, 2016), (Chollet, 2017), Densnet201 (Huang et al., 2017), Mobilenet v2 (Sandler et al., 2018) and Shufflenet (Zhang, Zhou, Lin, Sun, 2018). If one passes an image through the network and stops the network's evolution before the classification step, one obtains feature vectors for that image. Thus, we obtain ten sets of feature vectors, for each set we performed the classification process.

For clustering purposes, we used for feature extraction only five of the above mentioned networks: Resnet18, Resnet50, VGG16, InceptionResnet v2 and Densenet201.

Besides the five networks mentioned above, we also trained the following networks: VGG19, Mobilenet, Inception v3, Xception and Shufflenet.

For all these networks we performed data augmentation before training them and a 70%-30% split for the validation process. For augmentation translations and scaling were applied. We used a standard set of values for the usual parameters (batch size, learning rate). All the networks were trained under the same conditions. Our interest was to obtain good classification results with these networks, but our main goal was to test if the selection process performed on the dataset using clustering methods can improve the results obtained on the original dataset. The majority of tests were performed by using these ten networks for feature extraction and then employing linear SVM and Random Forest for classification. We also computed classification results using Resnet18 trained on some of the reduced training sets. We monitored if there are improvements of the performance evaluators.

As performance evaluators we used the accuracy (the percentage of correctly identified chest X-ray images from the total number of test images) and the Area Under the Curve ROC (Receiver Operating Characteristics), abbreviated AUC.

# 4 RESULTS

The experiments were performed on a laptop, with Intel(R) Core(TM) i7-8565U CPU, with a NVIDIA GeForce RTX 3060 GPU, in MATLAB 2020.

All the networks were trained 60 epochs, using the Stochastic Gradient Descent optimizer, mini batches of size 16, and cross-entropy loss function.

We adopted the following abbreviations for the clustering methods: E for 2-means with Euclidean distance, M – 2-means with Manhattan distance, C – complete linkage, A – average linkage, W – Ward linkage, S – spectral clustering.

All the results presented on this section are obtained on the test set, using the ten networks for feature extraction.

We began by computing the classification results using the original, unselected dataset, employing the trained neural networks, the linear SVM and Random Forest. For the last two classification methods we used the feature vectors produced by the same convolutional neural network, stopped before the classification layers. In Table 1 are the accuracies and in Table 2 the AUC values for these methods.

As expected, the trained networks provide the better results than the SVM and RF, Shufflenet producing the best overall result.

Table 1: Classification results on the original dataset: accuracies (%).

| Method | Network | SVM | RF |
|---|---|---|---|
| Resnet18 | 94.87 | 85.58 | 89.90 |
| Resnet50 | 94.07 | 91.35 | 89.74 |
| VGG16 | 94.23 | 89.58 | 89.90 |
| VGG19 | 96.63 | 88.46 | 90.87 |
| Densenet | 96.47 | 93.59 | 92.15 |
| Mobilenet | 95.03 | 92.15 | 90.38 |
| Inception | 94.53 | 93.11 | 91.51 |
| Xception | 95.51 | 90.87 | 89.42 |
| IncResnet | 94.87 | 91.99 | 91.83 |
| Shufflenet | 96.79 | 91.99 | 89.26 |

Table 2: Classification results on the original dataset: AUC values.

| Method | Network | SVM | RF |
|---|---|---|---|
| Resnet18 | 0.9367 | 0.8628 | 0.8654 |
| Resnet50 | 0.9243 | 0.8855 | 0.8632 |
| VGG16 | 0.9256 | 0.8628 | 0.8662 |
| VGG19 | 0.9576 | 0.8470 | 0.8791 |
| Densenet | 0.9572 | 0.9171 | 0.8970 |
| Mobilenet | 0.9380 | 0.8962 | 0.8726 |
| Inception | 0.9551 | 0.9107 | 0.8876 |
| Xception | 0.9444 | 0.8808 | 0.8624 |
| IncResnet | 0.9367 | 0.8966 | 0.8936 |
| Shufflenet | 0.9623 | 0.8940 | 0.8585 |

After performing the selection process described in the previous section, we were interested to see how many images in each class were selected. The new dimensions for the new training set classes are shown in Table 3. The first number in the cell is the number of normal chest X-ray images selected and the second is those with pneumonia. Note that all the clustering methods and networks select the great majority of the normal images in the first class. The complete and average linkage have difficulties in distinguishing between normal and pneumonia affected lungs. The VGG19 network has a good selection capability, regardless of the clustering method. We consider a good selection one that produces a pneumonia class that has at least 2500 images.

We performed classification tests using all the clustering methods and all the 10 types of deep learning generated features, with both SVM and RF. Table 4 and Table 5 show the best classification results obtained and the average accuracies for the five clustering method we tested. For the best results we show the accuracy value, the network that produced the feature vectors for classification and the

network that produced the feature vectors for the selection process. The average value is over the accuracies produced with the five networks employed in our computations for reducing the training set, for each clustering method. Table 4 shows the results obtained using the linear SVM classifier and Table 5 present the results for RF.

Table 3: New sizes of the dataset after the unsupervised selection process.

| | E | M | C | A | W | S |
|---|---|---|---|---|---|---|
| Resnet18 | 1349/ 2816 | 1349/ 3259 | 1349/ 739 | 1349/ 26 | 1349/ 2440 | 1307/ 146 |
| Resnet50 | 1346/ 2431 | 1342/ 3338 | 1345/ 6 | 1348/ 0 | 1345/ 2176 | 1244/ 293 |
| VGG19 | 1347/ 3796 | 1347/ 3765 | 1342/ 3864 | 1338/ 3869 | 1342/ 3870 | 1007/ 973 |
| IncResnet | 1341/ 3597 | 1342/ 3709 | 1349/ 5 | 1349/ 1 | 1348/ 19 | 1348/ 17 |
| Densenet | 1347/ 3550 | 1347/ 3673 | 1348/ 1214 | 1349/ 1 | 1334/ 3869 | 1246/ 366 |

Table 4: SVM results for different clustering techniques.

| | Best | | | Average |
|---|---|---|---|---|
| | Accuracy | Feat net | Selection | |
| E | 96.79% | VGG19<br>Densenet | Resnet50<br>Resnet18 | 94.79% |
| M | 96.31% | VGG16<br>Densenet<br>Shufflenet | Resnet18<br>Resnet18<br>Resnet18 | 94.34% |
| C | 96.96% | VGG16<br>Densenet<br>Inception | Densenet<br>Densenet<br>Densenet | 78.59% |
| A | 93.91% | Densenet | VGG16 | 57.66% |
| W | 97.12% | VGG16<br>Densenet | Resnet18<br>Resnet18 | 90.75% |
| S | 96.96% | Densenet | Resnet18 | 90.71% |

Table 5: RF results for different clustering techniques.

| | Best | | | Average |
|---|---|---|---|---|
| | Accuracy | Feat net | Selection | |
| E | 96.31% | Densenet | Resnet50 | 93.25% |
| M | 95.51% | VGG19 | Resnet18 | 92.43% |
| C | 96.79% | VGG19 | Resnet18 | 75.09% |
| A | 92.63% | VGG19<br>Densenet | Resnet18<br>VGG16 | 53.88% |
| W | 96.15% | Densenet | Resnet50 | 87.06% |
| S | 96.63% | Resnet18<br>Mobilenet<br>Inception | Resnet18<br>Densenet<br>Resnet17 | 88.58% |

We then studied which type of network employed for feature extraction provided the best classification result for each clustering method. In Table 6 are this type of dependency using the SVM classifier, and in Table 7 are the results for the RF. We use the following abbreviations for the five networks employed in the selection process: R18 and R50 for Resnet18 and Resnet50, respectively, D for Densenet, IR for InceptionResnet.

Note that certain clustering methods favour certain selection networks. For example, the 2-means clustering and Ward agglomerative method favour the Resnet class selection networks for both SVM and RF. Complete linkage favours features extracted with Densenet and average linkage prefers the VGG16 network. One notes that in these tables the InceptionResnet selection does not appear. The results presented in these two table are similar but not identical. From these tables one can deduce that a good choice for feature extraction in the selection process is a network from the class Resnet.

Table 6: Networks that provided best SVM accuracy results for each clustering method.

| | E | M | C | A | W | S |
|---|---|---|---|---|---|---|
| Resnet18 | R50 | R18 | D | Vgg16 | R50 | R18 |
| Resnet50 | R18 | R18 | D | Vgg16 | R18 | R50 |
| VGG16 | R50 | R18 | D | Vgg16 | R18 | R50 |
| VGG19 | R50 | Vgg16 | D | Vgg16 | R18 | R18 |
| Densenet | R18 | R18 | D | Vgg16 | R18 | R18 |
| Mobilenet | R18 | R18 | D | Vgg16 | R50 | R18 |
| Inception | R50 | R18 | D | Vgg16 | R50 | D |
| Xception | R18 | R18 | D | Vgg16 | R18 | R18 |
| IncResnet | R18 | R18 | D | Vgg16 | R50 | R50 |
| Shufflenet | R18 | R18 | D | Vgg16 | R18 | R50 |

Table 7: Best RF accuracy results for each clustering method.

| | E | M | C | A | W | S |
|---|---|---|---|---|---|---|
| Resnet18 | R50 | R18 | D | Vgg16 | R18 | R18 |
| Resnet50 | R18 | R18 | D | Vgg16 | R18 | R50 |
| VGG16 | R50 | R18 | D | R18 | R50 | R18 |
| VGG19 | R18 | R18 | R18 | R18 | R18 | R18 |
| Densenet | R50 | R18 | R18 | Vgg16 | R50 | D |
| Mobilenet | R50 | R18 | D | Vgg16 | R18 | D |
| Inception | R50 | R18 | D | Vgg16 | R50 | R50 |
| Xception | R50 | R18 | R18 | Vgg16 | R50 | R50 |
| IncResnet | R50 | R18 | D | Vgg16 | R18 | D |
| Shufflenet | R50 | R18 | D | Vgg16 | R18 | D |

This choice will be more evident from Table 8, where the best accuracy results depending on the clustering method are presented. The best improvement in accuracy result (97.12%) was obtained by using SVM on a dataset selected with Resnet50 or Resnet18 features with Ward or spectral clustering, the classification feature computed with VGG16 or Densenet. Comparing these results with those in Table 1, we deduce that there is an overall significant improvement in accuracy. The same happens when comparing the AUC values.

Table 8: Networks that provided best SVM accuracy results for each clustering method.

| | SVM | | RF | |
|---|---|---|---|---|
| | Acc. | Clust met | Acc. | Clust met |
| Resnet18 | 96.15% | M | 96.63% | S |
| Resnet50 | 96.15% | W | 95.99% | S |
| VGG16 | 97.12% | W, S | 96.63% | C |
| VGG19 | 96.79% | E | 96.96% | C |
| Densenet | 97.12% | W | 96.15% | S |
| Mobilenet | 96.15% | E | 96.47% | S |
| Inception | 96.96% | C | 95.83% | C |
| Xception | 96.63% | E | 95.83% | S |
| IncResnet | 95.03% | E | 94.71% | E |
| Shufflenet | 96.63% | E | 95.99% | S |

We present in the next figures the confusion matrices for classification results obtained on the whole dataset and on datasets selected using different clustering methods.

We show the confusion matrices for the classifiers that provided the best results: Shufflenet, for the original dataset (see Fig. 2), Densenet (Fig. 3 and 4) and VGG16 for the selected dataset (Fig. 5). Because in the selection process the main reduction was performed on the class of pneumonia images, we expect that the improvement in accuracy is due to the decrease of the false positive.

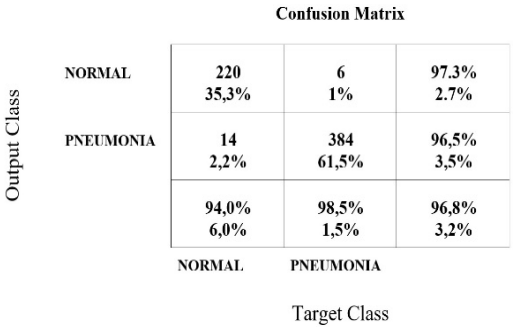


Figure 2: Confusion matrix for Shufflenet, trained on the original dataset.

We trained Resnet18 on different datasets selected with different networks for feature extraction and clustering methods. We chose those selected datasets that have enough images in the pneumonia class. The results (accuracy and AUC) are in Table 9. Almost in all situations the results are better than those obtained by training Resnet18 on the original, unselected dataset. For 2-means with Manhattan distance and feature extracted with Resnet50 we obtain the best overall result, 97.44%.

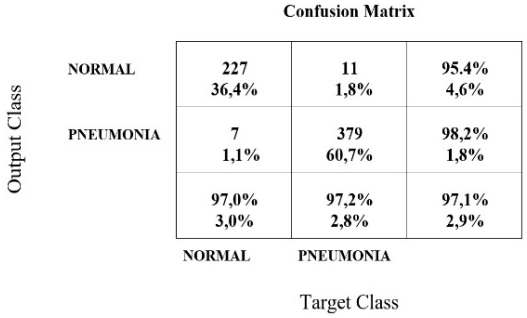


Figure 3: Confusion matrix for Densenet201, trained on the dataset selected with Resnet18 features and Ward clustering.

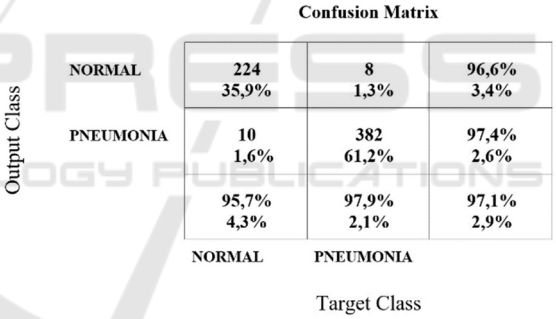


Figure 4: Confusion matrix for Densenet201, trained on the dataset selected with Resnet50 features and Ward clustering.

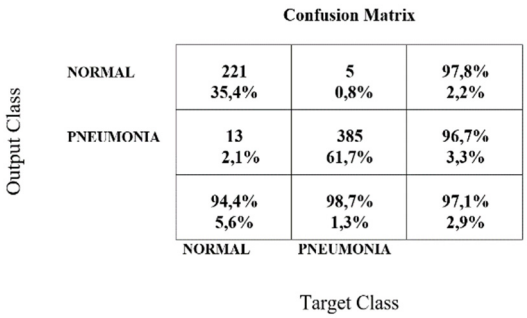


Figure 5: Confusion matrix for VGG16, trained on the dataset selected with Resnet18 features and Ward clustering.

Table 9: Resnet18 accuracy results obtained using training sets generated with different networks and clustering methods.

| | E | M | C | A | W |
|---|---|---|---|---|---|
| Resnet18 | 95.99%<br>0.962 | 96.79%<br>0.9658 | - | - | 86.38%<br>0.8868 |
| Resnet50 | 91.83%<br>0.9286 | **97.44%**<br>**0.9709** | - | - | 91.19%<br>0.9252 |
| VGG16 | 96.15%<br>0.9538 | 96.15%<br>0.9530 | 96.15%<br>0.9521 | 95.03%<br>0.9372 | 96.31%<br>0.9551 |
| IncResnet | 96.63%<br>0.9594 | 96.31%<br>0.956 | - | - | 96.96%<br>0.9654 |
| Densenet | 95.67%<br>0.9457 | 87.66%<br>0.8987 | 96.15%<br>0.9607 | - | 95.99%<br>0.956 |

In Figure 6 is the confusion matrix for the best results (Resnet18 trained on a training set selected with 2-means with Manhattan distance, with features produced by Resnet50). The false positives remain rather high, and this good result is due to the decrease of false negatives. We compared the results obtained with the same network, Resnet 18, but the training process was performed on the entire dataset. The confusion matrix is in Fig. 7. Note that the false negative are the same, the improvement of 2.5% in accuracy is due to the decrease of the false positive.

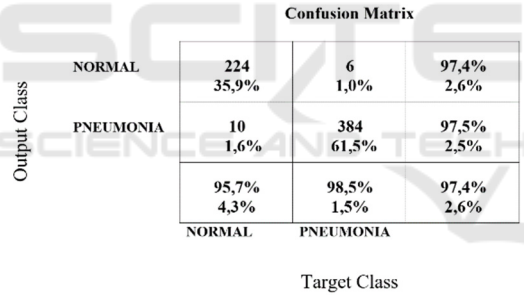


Figure 6: Confusion matrix for Resnet18, trained on the dataset selected with Resnet50 features and 2-means with Manhattan distance.

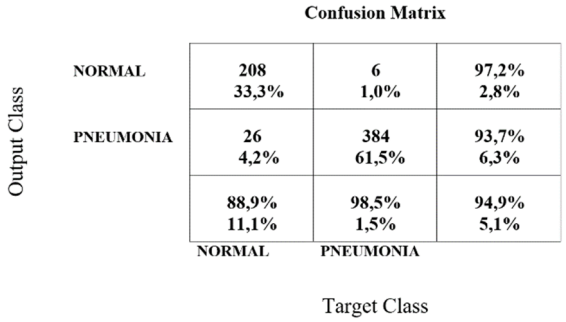


Figure 7: Confusion matrix for Resnet18, trained on the original dataset.

We compare our result with those obtained in other studies. Although there are articles that report classification results on the same dataset, in most of the cases the test set is not the same. The best results obtained for the same dataset, with the same split training-test as ours are in (Mabrouk et al., 2022) with accuracy 93.91% on the test set, and in (Chouhan, 2020) the reported accuracy is 96.39% with 0.9934 AUC. We could improve our results, by improving the results in Table 1. The results obtained in Table 1 can be improved by pre-processing the images in the original dataset, use a better augmentation procedure, and training the networks with different parameters (increasing the number of epochs, for example).

# 5 CONCLUSIONS

In this article, we tested the influence of clustering methods on the classification of chest X-ray image. We used three clustering techniques (with different underlying distances) to reduce the training set. In the same time, these unsupervised algorithms increased the training set's coherence, by deleting the inconsistent information. The feature extraction process was carried out with well-known CNNs, trained on the original dataset, with standard parameters. Linear SVMs, Random Forest and CNN methods provided the classification results. This blend of unsupervised with supervised learning computed better accuracy results on the Kermany dataset.

We intend to test this method on other datasets and with other clustering techniques. A pre-processing step can be added to the images in the dataset (histogram equalization, contrast enhancement, noise reduction) to improve the classification results. The method we presented tends to ignore the outliers, the non-standard CXR images. In order to address this problem, we plan to investigate the reformulation of this problem as a 3 or 4-class problem, by also using the images that now we eliminate from the training set, hoping to include in this new classes the atypical cases.

# REFERENCES

Lee, J. E., Kim, T. H., Cho, K. H., Han, K. T., & Park, E. C. (2017). The association between number of doctors per bed and readmission of elderly patients with pneumonia in South Korea. *BMC health services research*, *17*(1), 1-11.

Caseneuve, G., Valova, I., LeBlanc, N., & Thibodeau, M. (2021). Chest X-Ray Image Preprocessing for Disease Classification. *Procedia Computer Science*, *192*, 658-665.

Khan, W., Zaki, N., & Ali, L. (2021). Intelligent pneumonia identification from chest x-rays: A systematic literature review. *IEEE Access*, *9*, 51747-51771.

Çallı, E., Sogancioglu, E., van Ginneken, B., van Leeuwen, K. G., & Murphy, K. (2021). Deep learning for chest X-ray analysis: A survey. *Medical Image Analysis*, *72*, 102125.

Li, Y., Zhang, Z., Dai, C., Dong, Q., & Badrigilan, S. (2020). Accuracy of deep learning for automated detection of pneumonia using chest X-ray images: a systematic review and meta-analysis. *Computers in Biology and Medicine*, *123*, 103898.

Ayan, E., & Ünver, H. M. (2019, April). Diagnosis of pneumonia from chest X-ray images using deep learning. In *2019 Scientific Meeting on Electrical-Electronics & Biomedical Engineering and Computer Science (EBBT)* (pp. 1-5). Ieee.

Sharma, H., Jain, J. S., Bansal, P., & Gupta, S. (2020, January). Feature extraction and classification of chest x-ray images using cnn to detect pneumonia. In *2020 10th International Conference on Cloud Computing, Data Science & Engineering (Confluence)* (pp. 227-231). IEEE.

Kermany, D., Zhang, K. G. M., & Goldbaum, M. Large dataset of labeled optical coherence tomography (OCT) and chest x-ray images, Mendeley data, v3 (2018).

Hammoudi, K., Benhabiles, H., Melkemi, M., Dornaika, F., Arganda-Carreras, I., Collard, D., & Scherpereel, A. (2021). Deep learning on chest X-ray images to detect and evaluate pneumonia cases at the era of COVID-19. *Journal of medical systems*, *45*(7), 1-10.

Mabrouk, A., Díaz Redondo, R. P., Dahou, A., Abd Elaziz, M., & Kayed, M. (2022). Pneumonia Detection on Chest X-ray Images Using Ensemble of Deep Convolutional Neural Networks. *Applied Sciences*, *12*(13), 6448.

Kundu, R., Das, R., Geem, Z. W., Han, G. T., & Sarkar, R. (2021). Pneumonia detection in chest X-ray images using an ensemble of deep learning models. *Plos one*, *16*(9), e0256630.

Chouhan, V., Singh, S. K., Khamparia, A., Gupta, D., Tiwari, P., Moreira, C., ... & De Albuquerque, V. H. C. (2020). A novel transfer learning based approach for pneumonia detection in chest X-ray images. *Applied Sciences*, *10*(2), 559.

Zhang, Dejun, Fuquan Ren, Yushuang Li, Lei Na, and Yue Ma. "Pneumonia detection from chest X-ray images based on convolutional neural network." *Electronics* 10, no. 13 (2021): 1512.

Tan, P. N., Steinbach, M., & Kumar, V. (2019). *Introduction to data mining*. Pearson Education India, 2nd ed.

Landau, S., Leese, M., Stahl, D., & Everitt, B. S. (2011). *Cluster analysis*. John Wiley & Sons, 5th ed.

Wierzchoń, S. T., & Kłopotek, M. A. (2018). *Modern algorithms of cluster analysis* (Vol. 34). Springer International Publishing.

He, K., Zhang, X., Ren, S., & Sun, J. (2016). Deep residual learning for image recognition. In *Proceedings of the IEEE conference on computer vision and pattern recognition* (pp. 770-778).

Simonyan, K., & Zisserman, A. (2014). Very deep convolutional networks for large-scale image recognition. *arXiv preprint arXiv:1409.1556*.

Szegedy, C., Vanhoucke, V., Ioffe, S., Shlens, J., & Wojna, Z. (2016). Rethinking the inception architecture for computer vision. In *Proceedings of the IEEE conference on computer vision and pattern recognition* (pp. 2818-2826).

Chollet, F. (2017). Xception: Deep learning with depthwise separable convolutions. In *Proceedings of the IEEE conference on computer vision and pattern recognition* (pp. 1251-1258).

Huang, G., Liu, Z., Van Der Maaten, L., & Weinberger, K. Q. (2017). Densely connected convolutional networks. In *Proceedings of the IEEE conference on computer vision and pattern recognition* (pp. 4700-4708).

Sandler, M., Howard, A., Zhu, M., Zhmoginov, A., & Chen, L. C. (2018). Mobilenetv2: Inverted residuals and linear bottlenecks. In *Proceedings of the IEEE conference on computer vision and pattern recognition* (pp. 4510-4520).

Zhang, X., Zhou, X., Lin, M., & Sun, J. (2018). Shufflenet: An extremely efficient convolutional neural network for mobile devices. In *Proceedings of the IEEE conference on computer vision and pattern recognition* (pp. 6848-6856).